

AD-A098 349

HUGHES RESEARCH LABS MALIBU CA
ELECTRONIC PROCESSES IN IMP AND RELATED COMPOUNDS. (U)
FEB 81 K V VAIDYANATHAN, C L ANDERSON

F/G 20/13

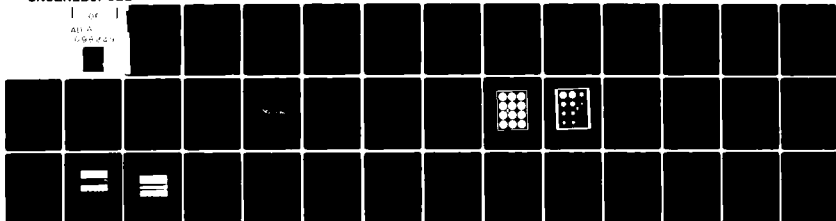
N00019-79-C-0533

NL

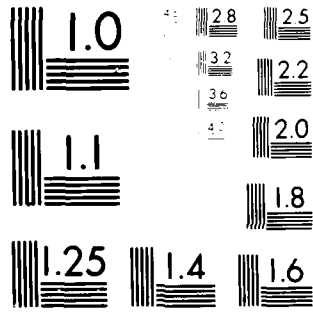
UNCLASSIFIED

1 of 1

AD-A
1086421



END
DATE
FILMED
5-81
DTIC



MICROCOPY RESOLUTION TEST CHART
NATIONAL BUREAU OF STANDARDS-1963-A

LEVEL

AD 88 446

12

5

AD A 098349

ELECTRONIC PROCESSES IN InP AND RELATED COMPOUNDS

K.V. Vaidyanathan, C.L. Anderson, H.L. Dunlap, D.E. Holmes and G.S. Kamath

Hughes Research Laboratories
3011 Malibu Canyon Road
Malibu, CA 90265

February 1981

Contract No. N00019-79-C-0533
Annual Report
13 August 1979 through 12 August 1980

Approved for public release; distribution unlimited.

Prepared for:
NAVAL AIR SYSTEMS COMMAND
Washington, DC 20361

+ DTIC FILE COPY

81 4 30 018

UNCLASSIFIED

SECURITY CLASSIFICATION OF THIS PAGE (When Data Entered)

REPORT DOCUMENTATION PAGE		READ INSTRUCTIONS BEFORE COMPLETING FORM
1. REPORT NUMBER	2. GOVT ACCESSION NO. AD-A098	3. RECIPIENT'S CATALOG NUMBER 349
6. TITLE (and Subtitle) ELECTRONIC PROCESSES IN InP AND RELATED COMPOUNDS		8. TYPE OF REPORT & PERIOD COVERED Annual Report, 13 Aug 1979 - 12 Aug 1980
7. AUTHOR(s) K.V. Vaidyanathan, C.L. Anderson, H.L. Dunlap, D.E. Holmes and G.S. Kamath		9. PERFORMING ORG. REPORT NUMBER
9. PERFORMING ORGANIZATION NAME AND ADDRESS Hughes Research Laboratories 3011 Malibu Canyon Road Malibu, CA 90265		10. CONTRACT OR GRANT NUMBER(s) N00019-79-C-0533
11. CONTROLLING OFFICE NAME AND ADDRESS Department of the Navy Naval Air Systems Command Washington, D.C. 20361		12. REPORT DATE February 1981
14. MONITORING AGENCY NAME & ADDRESS (if different from Controlling Office) 1240		13. NUMBER OF PAGES 39
16. DISTRIBUTION STATEMENT (of this Report) Approved for public release; distribution unlimited.		15. SECURITY CLASS. (of this report) UNCLASSIFIED
17. DISTRIBUTION STATEMENT (of the abstract entered in Block 20, if different from Report)		15a. DECLASSIFICATION DOWNGRADING SCHEDULE
18. SUPPLEMENTARY NOTES		
19. KEY WORDS (Continue on reverse side if necessary and identify by block number) Ionization coefficient measurements Liquid phase epitaxy of InP		
20. ABSTRACT (Continue on reverse side if necessary and identify by block number) The growth and characterization of high-purity epitaxial layers grown by liquid-phase-epitaxy (LPE) are described. Chemical and electrical evaluation of the layers indicate that silicon and sulfur are the dominant residual donors in LPE-grown InP layers. Techniques for controlling these dopants are discussed.		

DD FORM 1473 EDITION OF 1 NOV 65 IS OBSOLETE

UNCLASSIFIED

SECURITY CLASSIFICATION OF THIS PAGE (When Data Entered)

172600

11

UNCLASSIFIED

SECURITY CLASSIFICATION OF THIS PAGE (When Data Entered)

The current-voltage characteristics of Schottky diodes on p-InP are analyzed. Aluminum, silver, and gold were tried as Schottky-barrier metals. The results reported here demonstrate that Al is the best choice as the Schottky metal. An automated system to measure the relative photoresponse from Schottky diodes has been assembled. Majority carrier (hole) initiated avalanche multiplication has been observed on these Schottky diodes.

UNCLASSIFIED

SECURITY CLASSIFICATION OF THIS PAGE (When Data Entered)

TABLE OF CONTENTS

SECTION		PAGE
1	INTRODUCTION	6
2	EPITAXIAL GROWTH OF InP	8
3	DEVICE STRUCTURE DEVELOPMENT	18
4	IONIZATION COEFFICIENT MEASUREMENTS	29
	A. Design of the Experimental System to Perform Ionization Coefficient Measurements	29
	B. Experimental Measurements	31
5	SUMMARY	37
	REFERENCES	39

Accession For	
NTIS GRA&I	<input checked="" type="checkbox"/>
DTIC TAB	<input type="checkbox"/>
Unannounced	<input type="checkbox"/>
Justification	
By _____	
Distribution/	
Availability Codes	
Dist	Avail and/or Special
A	

LIST OF ILLUSTRATIONS

FIGURE		PAGE
1	Liquid phase epitaxial growth system	9
2	Epilayer doping concentration versus distance profiles at various points on the wafer shown in the inset	10
3	Graphite slide-bar assembly	11
4	Photoluminescence spectra of InP	14
5	Secondary ion mass spectrometry (SIMS) profiles of silicon in InP epitaxial layers	16
6	First level mask to define Ohmic contacts for fabricating guarded Schottky diodes in InP	20
7	Second level mask to define the Schottky and guard ring in InP	21
8	Current-voltage characteristics of 400- μ m-diameter reverse-biased Schottky diodes on p-InP	23
9	Current-voltage characteristics of forward-biased Schottky diodes on p-InP. The Schottky metal was Al	24
10	Current-voltage characteristics (forward bias) of Au Schottky diodes on p-InP	25
11	Current-voltage (forward) characteristics of Ag-Schottky diodes on p-InP	26
12(a)	SEM micrograph of a mesa etched in InP with mechanically gaited 2% solution of bromine in methanol	27
12(b)	SEM micrograph of a mesa in InP produced by jet thinning with 2% solution of bromine in methanol	28
13	Schematic of the automated photoresponse measurement system	30
14	The measured photocurrents as a function of reverse bias from a 400 μ m diameter Schottky diode on p-InP	32
15	Normalized photocurrent due to 1.152 μ m illumination on p-InP	33

FIGURE		PAGE
16	Hole-initiated avalanche multiplication factor obtained from p-InP diodes	34
17	Normalized photocurrent caused by 0.6328 μm illumination on p-InP	35

SECTION 1

INTRODUCTION

Optical fibers capable of functioning in long-base line, high-speed, secure communication systems have been developed. Recent progress in optical fiber technology has resulted in the development of radiation-resistant optical fibers with very low attenuation and very low dispersion in the 1.0 to 1.5 μm wavelength range. Such systems are immune to electromagnetic interference and can be used in high-radiation environments. To exploit this technology, it is necessary to develop semiconductor photoemitters (lasers or light-emitting diodes) and photodetectors capable of operating in this wavelength range as well as amplifiers, logic circuits, and signal processing circuits. High-speed operation requires development of avalanche or p-i-n photodiodes as detectors. Either type of detector has its own specific advantages and disadvantages. It is also clear that no simple homopolar or binary compound semiconductor is well suited to cover all the above requirements. InGaAs and InGaAsP compounds, which can be grown lattice matched on InP substrates with the appropriate bandgap, appear to be the ideal materials candidates to satisfy the goals mentioned above.

The relative magnitudes of the ionization coefficient of electrons (α), and of holes (β), play an important role in the optimal design of avalanche photodiodes. The basic device configuration will depend on the values of α and β , since for lowest noise, the carrier with the highest ionization coefficient must be injected into the avalanche region. The major goals of this experimental program are to develop techniques for measuring the photo-multiplied currents in suitable device structures and to analyze the data to yield the ionization coefficients of electrons and holes as a function of the electric field in InP and related ternary and quaternary compounds.

The work carried out during this reporting period is divided into four major areas:

- Growth of high purity InP layers by liquid-phase epitaxy (LPE) using our patented infinite-solution growth technique, to characterize the grown layers, and to extend the technique to the growth of ternary (In, Ga)As and the quaternary (In, Ga)(As, P) compounds.

- Development of device structures exhibiting abrupt reverse breakdown characteristics, free of microplasmas and exhibiting avalanche gains so that photocurrent measurements can be performed as a function of electric field. The electric field distribution is accurately known in Schottky barrier devices. We therefore believe that Schottky devices would be the most appropriate structure for performing these measurements. To develop such structures, we have investigated the current-voltage characteristics of Schottky diodes using different metals and have obtained barrier heights for these metals on p-type InP. The choice of p-InP is dictated because of unacceptable low Schottky barrier heights on n-type InP.
- Design and construction of an automated system capable of measuring photomultiplied currents due to pure electron- and pure hole-injection in the high-field region of the test structure. In this case, the electron- and hole-injection is obtained by illuminating the device from the backside with highly absorbing ($0.6328 \mu\text{m}$) and essentially transparent ($1.152 \mu\text{m}$) radiation, respectively. This procedure is advantageous since the same device structure is used to achieve the required carrier injections.
- Investigation of methods of obtaining accurate nonmultiplied photocurrents as a function of the electric field in the device and to analyze the data to yield the ionization coefficients.

The report describes the progress made in each of these areas and describes the work to be performed during the second phase of this program.

SECTION 2

EPITAXIAL GROWTH OF InP

InP, (In, Ga)As, and (In, Ga)(As, P) layers can be epitaxially grown by a variety of techniques such as liquid-phase epitaxy (LPE),¹ vapor phase epitaxy (VPE),² metal organic chemical vapor deposition (MOCVD),³ planar reactive deposition (PRD),⁴ and molecular beam epitaxy (MBE).⁵ It appears that LPE, offers the best potential for the growth of high-purity InP at this stage.

Two variations of the LPE technique are commonly used: the slide-bar technique using small solutions (the limited melt technique) and the dipping technique using larger solutions (the infinite solution technique). The slide-bar technique has the disadvantage that severe melt depletion effects can occur. Consequently, only a few layers with reproducible properties can be grown from a single melt. This may be a potential problem in the growth of ternary and quaternary layers. In contrast, the infinite solution technique, in principle, permits several hundred layers with reproducible properties to be grown from the same melt.

Hughes Research Laboratories (HRL) has developed a unique variation of the infinite solution growth technique. This variation, illustrated in Figure 1, consists basically of an all-quartz growth tube connected by a high-vacuum valve to a stainless-steel entry chamber. A saturated solution of the appropriate elements serves as the growth matrix. Once a specific solution has been prepared, it is kept in a palladium-purified hydrogen ambient. It can thus be maintained at or near the growth temperature in a controlled environment for months. During a long series of runs, all epitaxial growth operations (such as introducing substrates or adding dopants) are performed by passing these materials through an entry chamber, which can be independently evacuated and flushed with hydrogen before opening to the growth tube. It is thus possible to maintain a high-purity solution for a period of months. The growth ambient can also be conveniently changed while all other variables are kept under control. This capability is extremely advantageous in growing high-purity InP layers and is discussed in detail later in this section.

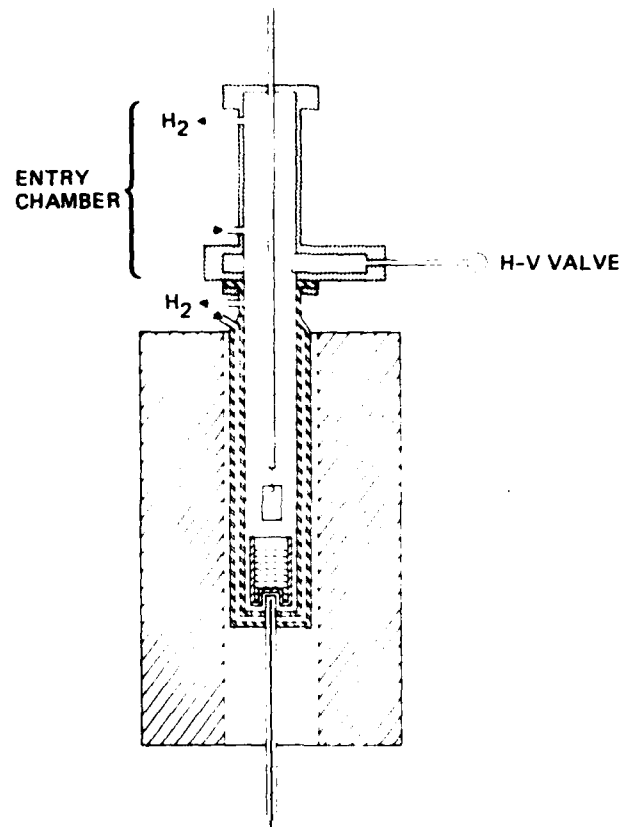


Figure 1. Liquid phase epitaxial growth system.

Figure 2 shows the variation in doping concentration as a function of distance into the epitaxial layer at various points over a large Sn-doped wafer (1 x 1-1/4 in., shown in insert). This represents the doping homogeneity that can be obtained in layers grown by the infinite solution system.

The performance of optoelectronic devices depends critically on the ability to grow uniform, thin, homogeneous and dislocation-free epitaxial layers. Also, in devices involving heterojunctions, it is necessary to reduce defects at the interface. To satisfy all these requirements, the surfaces must see a uniform growth ambient (a chemically homogeneous growth matrix and uniform temperature over the growth surface), and the layers must be grown slowly enough to permit near-equilibrium conditions to be established at the growth interface.

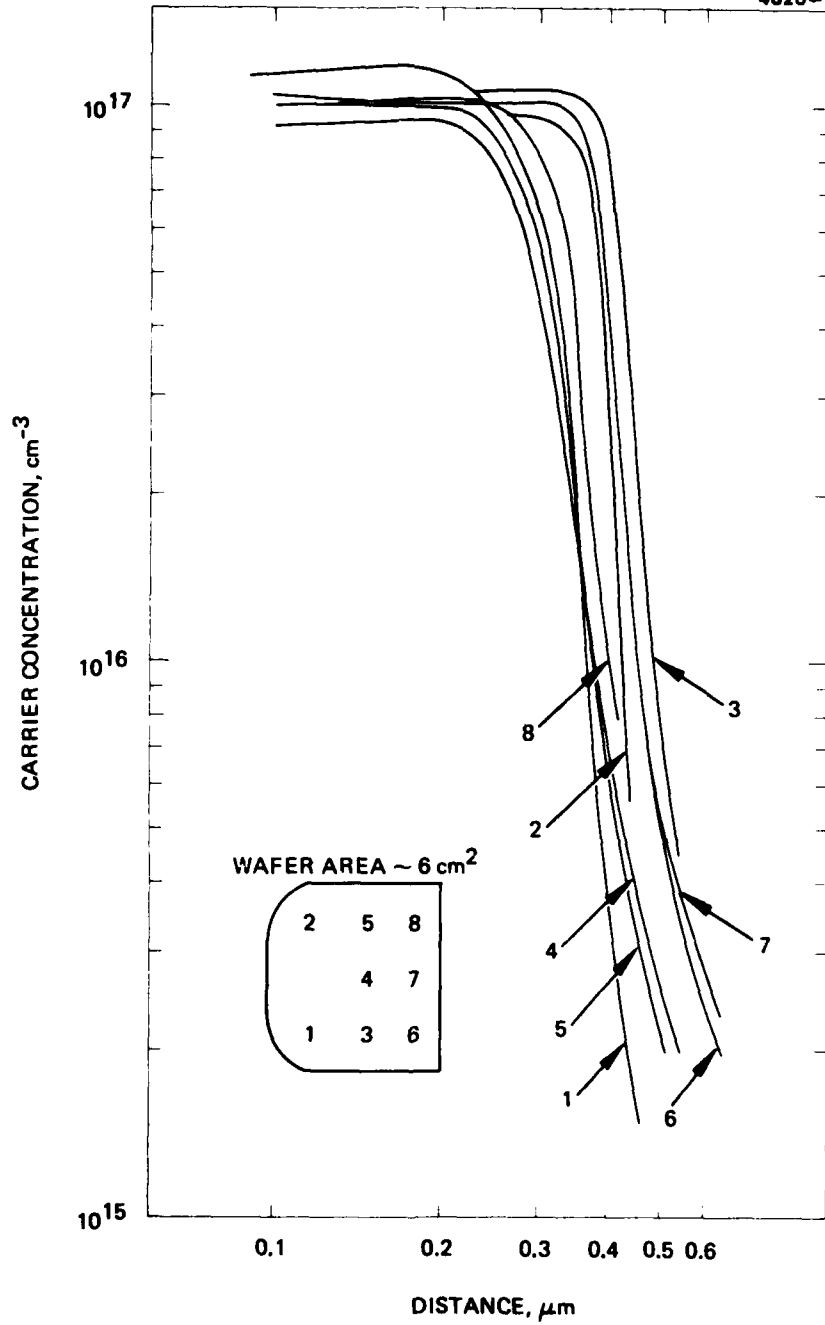


Figure 2. Epilayer doping concentration versus distance profiles at various points on the wafer shown in the inset.

We have developed a graphite sample holder assembly to house the substrate (Figure 3) that permits us to operate under such conditions. The substrate is introduced into the melt within the sample holder, and the whole assembly rotates in the melt until temperature equilibrium is fully established. This rotation further helps to ensure good mixing and homogeneity in the melt. By raising the graphite cover, the sample is exposed to the melt. Growth is stopped by (1) closing the cover; (2) raising the sample holder out of the solution; and (3) reopening the cover, at which point the solution trapped in the sample holder falls out. Note that at no time in the growth procedure does the surface of the sample pass through the meniscus on the solution. Furthermore, the cover of the sample holder does not wipe the melt from the sample. Using this technique, we have grown thin epitaxial layers with excellent surface morphology and reproducible electrical properties.

The infinite solution technique has been successfully used to grow high-purity InP layers with carrier concentrations of $\sim 3 \times 10^{15} \text{ cm}^{-3}$ and mobilities of $4,500 \text{ cm}^2 \text{ V}^{-1} \text{ sec}^{-1}$ (77°K mobility of $41,000 \text{ cm}^2 \text{ V}^{-1} \text{ sec}^{-1}$)

4107 10

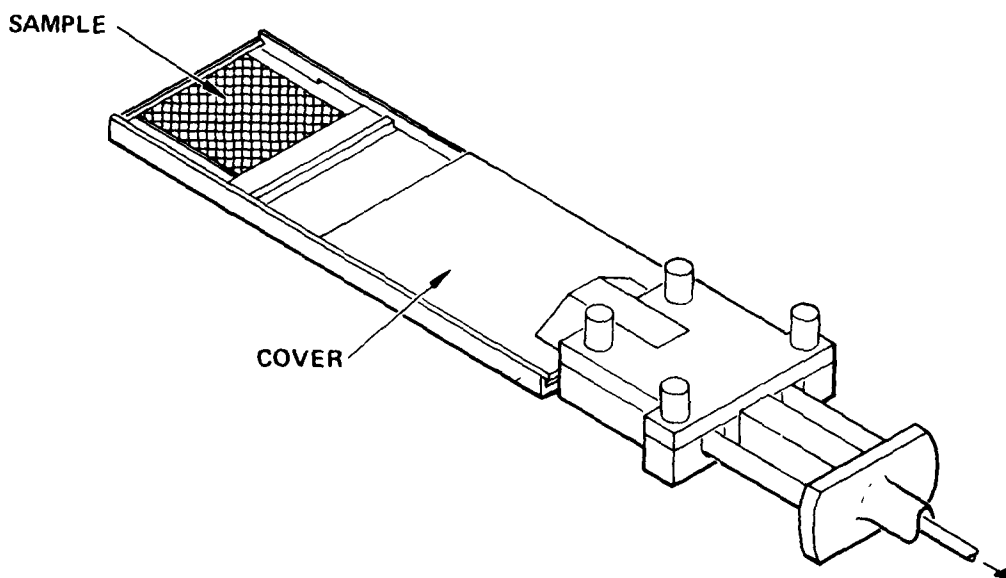


Figure 3. Graphite slide-bar assembly.

reproducibly. We have also conducted extensive studies, using internal funds, to study the influence of 0.1 to 10 ppm of water vapor in the growth ambient. The results of this study are summarized in Table 1. These results can be explained as follows. Silicon is believed to be the dominant residual donor in InP. The quartz in the growth system reacts with H_2 , which reduces it to SiO vapor. The SiO vapor is then reduced by In in solution, which results in Si doping of the solution. Consequently, in the presence of pure H, the Si level in solution reaches an equilibrium level. However, when a small quantity of water vapor is added to the growth ambient, the reduction of quartz by H is suppressed; also, the Si in solution reacts with water vapor, forming SiO vapors. Consequently, the Si level in solution is reduced considerably. This model has been verified by experiments in which layers were grown by turning the water vapor on and off. Under those conditions, net donor concentration cycles: it is high when water vapor is absent and low when it is present.

Extensive Hall-effect measurements have been performed as a function of temperature on the epitaxial layers. Analysis of the data yields the donor (N_D) and acceptor (N_A) concentrations and the degree of compensation. The data clearly show that both N_D and N_A decrease when even small quantities of water vapor are present in the growth ambient. Since Si is the dominant residual impurity, we believe, this evidence indicates the amphoteric nature of Si in InP. This is the first time that the acceptor behavior of Si in InP has been observed. In contrast to the situation with GaAs, this effect is observable in InP only at very low Si concentrations. This, we believe, is a good example of the purity of our epitaxial layers.

The results of a low-temperature photoluminescence (PL) evaluation of InP epitaxial layers grown in the absence and presence of water vapor in the growth ambient are shown in Figure 4. The sample grown in pure H had a total carrier concentration of $8.5 \times 10^{16} \text{ cm}^{-3}$. The PL spectrum obtained from this sample is dominated by broad emission bands at 1.419 eV and 1.385 eV. The 1.419 eV band is related to bandedge emission and is relatively broad in this sample. The emission at 1.385 eV appears to involve donors and acceptors. In contrast, the spectrum from a sample grown in the presence of water vapor exhibits

Table 1. Electrical Properties of InP Epitaxial Layers Illustrating the Influence of Water Vapor in the Gas Stream

Sample Number	Ambient	n, cm^{-3} (300°K)	$\mu, \text{cm}^2 \text{V}^{-1}$ sec^{-1} (300°K)
1	Pure hydrogen	1.4×10^{17}	2600
2	Pure hydrogen	2.6×10^{17}	2600
3	Hydrogen + H ₂ O	2.1×10^{15}	3500
4	Hydrogen + H ₂ O	2.3×10^{15}	4500
5	Hydrogen + H ₂ O	4.2×10^{15}	4200
6	Hydrogen + H ₂ O	2.3×10^{15}	3800
7	Hydrogen + H ₂ O	2.5×10^{15}	4100
8	Hydrogen + H ₂ O	2.9×10^{15}	4100
9	Pure hydrogen	1.1×10^{16}	3700
10	Pure hydrogen	6.1×10^{16}	3100
11	Pure hydrogen	1.1×10^{17}	3200
12	Hydrogen + H ₂ O	2.3×10^{15}	4200

6559

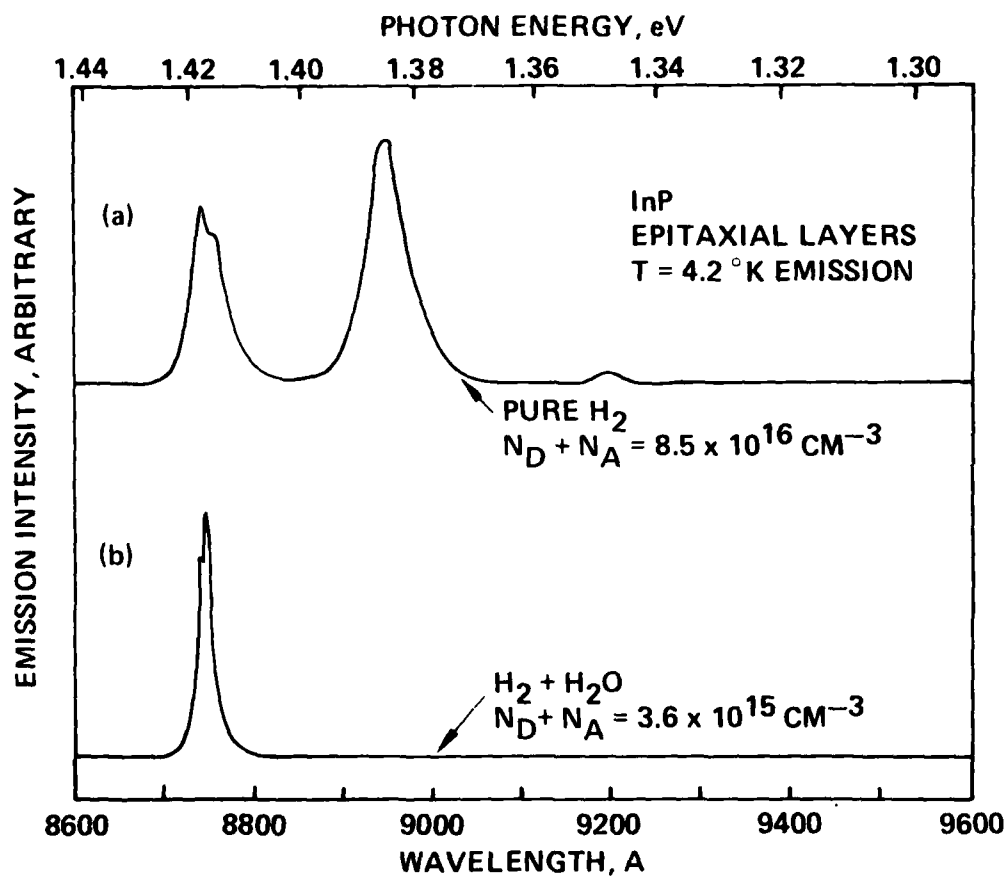


Figure 4. Photoluminescence spectra of InP.

a narrower edge emission (1.419 eV) and an absence of the donor-acceptor emission. The electrical and optical evaluations discussed above show that the samples grown in the presence of water vapor are in fact of higher purity than the ones grown in a H ambient (with no water vapor present).

We have also performed secondary ion mass spectrometry (SIMS) studies on InP liquid epilayers grown in H ambient as well as in samples grown in the presence of water vapor. By using Cs ions as the primary bombarding species, it has been demonstrated that the detection sensitivity for Si and other group IV elements can be improved. As seen from the data in Figure 5, it is clear that layers grown in the presence of water vapor contain smaller quantities of Si as an impurity. Similar results were also obtained from Auger electron spectroscopy (AES) studies. The chemical studies mentioned above, in conjunction with the electrical data presented earlier, clearly demonstrate that the incorporation of Si resulting from the reduction of quartz is indeed an important source of donors in LPE-grown InP.

During the course of these investigations, we observed that not all solutions responded in the same fashion (quantitatively) to the addition of water vapor. Carrier concentrations ~ 2 to $3 \times 10^{16} \text{ cm}^{-3}$ were measured when layers were grown from some solutions in the presence of water vapor in the growth ambient. These results led us to believe that an additional donor may be present in the starting solution and consequently get incorporated in the grown layers. Detailed mass spectrometry analysis of such layers reveal the presence of considerable quantities of S. The S contamination may either be associated with the starting polycrystalline material or may be caused by some other source of contamination, such as the graphite sample holder. We are now investigating the source of the S contamination.

Since the vapor pressure of S is quite high, it is possible to reduce the S contamination by baking one growth solution at higher temperatures. Following such a bake-out and by performing the growth at a temperature lower than the bakeout temperature, in the presence of water vapor in the growth ambient, high purity InP layers can be grown even from a contaminated solution.

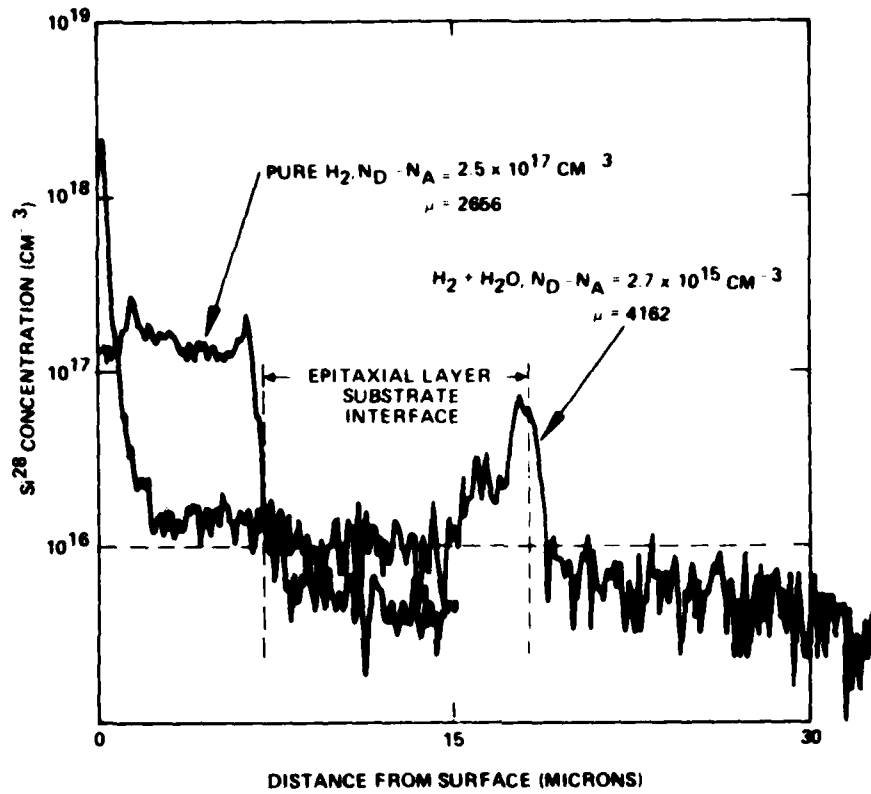


Figure 5. Secondary ion mass spectrometry (SIMS) profiles of silicon in InP epitaxial layers. Layer grown in the presence of water vapor contains small quantities of silicon while a layer grown in pure hydrogen ambient contains large quantities of silicon.

After establishing the criterion for high-purity growth, we will counterdope the solution with controlled quantities of acceptors to result in the growth of lightly doped p-type layers with hole mobilities in excess of $100 \text{ cm}^2 \text{ V}^{-1} \text{ sec}^{-1}$. To grow several layers with reproducible properties, it is necessary to choose an acceptor exhibiting low vapor pressure. We have successfully demonstrated that p-type GaAs and (Al, Ga)As layers can be grown using either Be or Ge as an acceptor dopant. We will use either one of them as a dopant of choice for the growth of p-type InP.

A second growth furnace is now being designed and assembled. It will be dedicated to the ternary (In, Ga)As growth and will be available for use in 1981.

SECTION 3

DEVICE STRUCTURE DEVELOPMENT

In the design of avalanche photodiodes, it is necessary to know the relative magnitudes of the electron and hole ionization coefficients $\alpha(E)$ and $\beta(E)$, respectively. By injecting the carrier with the highest ionization coefficient in the high-field region of the device to initiate the multiplication event, photodiodes exhibiting high avalanche gain as well as having a large bandwidth and excellent signal-to-noise ratio can be fabricated.

The ionization coefficients effectively describe the interaction and multiplication of electrons and holes in the high field of the region of the semiconductor. It is essential that the device structures used for performing these measurements be capable of sustaining high electric fields and be free from local regions suffering from premature breakdown. It is also necessary that these devices be designed for efficient collection of light and the rapid transport of the photogenerated carriers to the high-field region of the device. Either Schottky barrier or p-n junction diodes can be used as suitable device structures. As pointed out earlier, breakdown resulting from inhomogeneties in the sample (microplasmas) or surface breakdown effects should be prevented in the device structure. Typically, surface breakdown effects can be minimized by suitable Schottky barrier guard rings or by shaping the mesas in mesa junction devices.

In addition to these requirements, Chynoweth⁶ has pointed out some of the conditions to be satisfied in an ideal ionization coefficient measurement experiment:

- Pure electron or hole injection should be used in the same junction rather than complementary junctions.
- The profile and magnitude of the field in the junction region should be accurately known.
- The structures should be free from microplasmas over the bias range used in the measurements.

The first two of the Chynoweth criteria can be satisfied by using a Schottky barrier with appropriate optical injection of electrons and holes in the high-field region of the device. The fabrication and properties of Schottky barrier device structures are described below.

To fabricate guarded Schottky diodes, we have designed a versatile and yet simple mask set. Figure 6 shows the first level in this mask set. This mask will permit us to form ohmic contacts on the front surface of the device. After a photolithographic liftoff has been completed with this mask, the ohmic contact metal will cover the wafer except for the regions corresponding to the dark circles on the mask. Figure 7 shows the second level of the mask, which will permit us to define the Schottky barrier and the guard ring metalization in one photolithographic step. Two different spacings between the Schottky barrier and the guard ring (3 and 10 μm) are available. Also, diodes with diameters of 400, 200, 100 and 50 μm can be fabricated. Diodes with no guard ring are also available as test devices. By using an appropriate polarity of the mask shown in Figure 6, the region underneath the ohmic contact can be heavily doped by ion implantation while maintaining the doping level underneath the Schottky at acceptable low levels. There is also a provision for performing selective area implantation to form planar p-n junction structures by ion implantation. This feature will permit us to fabricate p^+-n or n^+-p junction diodes along with the Schottky diodes as test structures.

Using the mask set discussed above, we have fabricated and evaluated Schottky diodes on p-type InP. The p-InP samples were lightly doped ($\sim 6 \times 10^{15}$ holes/cm³) and were obtained from Varian Associates. They were chemimechanically polished in 2% solution of Br in methanol to yield smooth scratch-free surfaces. They were further free etched in a solution of 1:1:1:6, perchloric acid (HClO₄:HCl:acetic acid (H Ac):HNO₃). Ohmic contacts were formed by sputter depositing Au-Zn alloy followed by alloying at 480°C for one minute.

To prevent decomposition of the InP surface during the high temperature alloying process, the samples were covered with SiO₂ encapsulant layer. Acceptable ohmic contacts with little or no surface degradation were formed by this process. To decrease the contact resistance further, it will be necessary to increase the doping level underneath the contacts by performing Be-ion implantation. Schottky barrier diodes were fabricated by evaporating either Al, Ag, or Au as the Schottky metal and their I-V characteristics were evaluated.

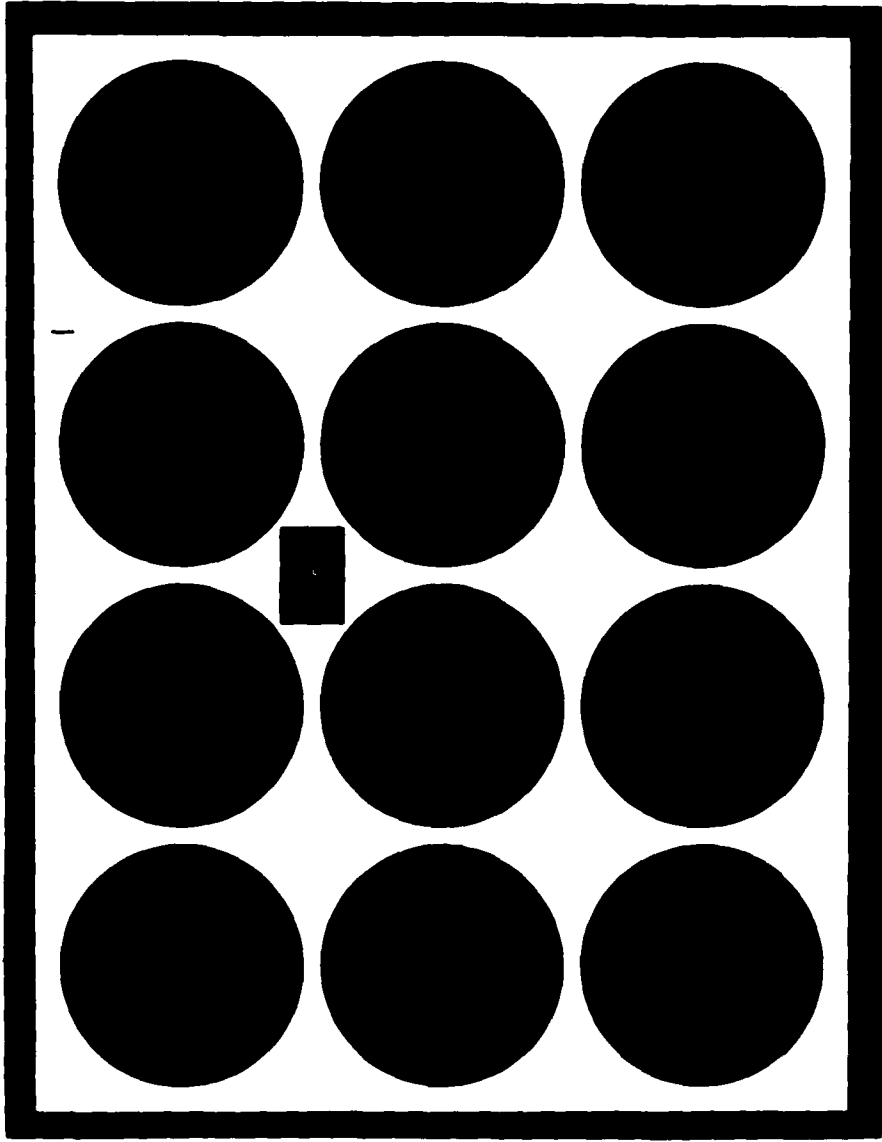


Figure 8 illustrates the I-V characteristics in the reverse direction of Al Schottky diodes on p-InP. The leakage current, as seen from the figure, is quite low even at reverse bias voltage of 20 V. The breakdown is abrupt, and there appears to be no problem associated with microplasma. Even in the presence of external illumination, the reverse leakage current is quite low. The forward I-V characteristics obtained for Al Schottky diode with different diameters is shown in Figure 9. The I-V curves can be described by the classic relation.

$$J = A^* T^2 e \frac{q\phi_B}{kT} \left[\exp\left(\frac{qV}{nkT}\right) - 1 \right] .$$

where A^* is the Richardson's constant, T is the absolute temperature, $q\phi_B$ is the Schottky barrier height in eV, V is the applied voltage, and n is the ideality factor. For Al on p-InP, we estimate the Schottky barrier height to be 0.9 eV and the ideality factor to be 1.059. The I-V characteristics in the forward direction for Au and Ag Schottky diodes are shown in Figures 10 and 11, respectively. Analysis of the data indicates that the Schottky barrier height of Au on p-InP is ~ 0.64 eV, while the ideality factor is 1.3. Previously published data indicate that the barrier height of Au on p-InP maybe ~ 0.76 eV. For Ag, we estimate the barrier height to be between 0.74 and 0.81 eV and the ideality factor to be ~ 1.5 . From this study, it is clear that Al forms an ideal Schottky barrier on p-InP and will be the baseline approach in our Schottky diode fabrication. Analysis of the data also reveals that the reverse leakage currents in both directions scale with the area of the device. This indicates that the origin of the observed leakage currents arises from the bulk of the crystal.

To perform the ionization coefficient measurements, it is necessary to thin the samples so that almost all of the photogenerated carriers are injected into the high-field region and are not lost by recombination. Since the samples have to be self-supporting, it is necessary to selectively thin a portion of the sample. When the sample is etched in a solution that is mechanically stirred or agitated, the typical etch region with a moat around the edge is obtained and is shown in Figure 12(a). However, when a jet of the etchant solution is directed at the sample

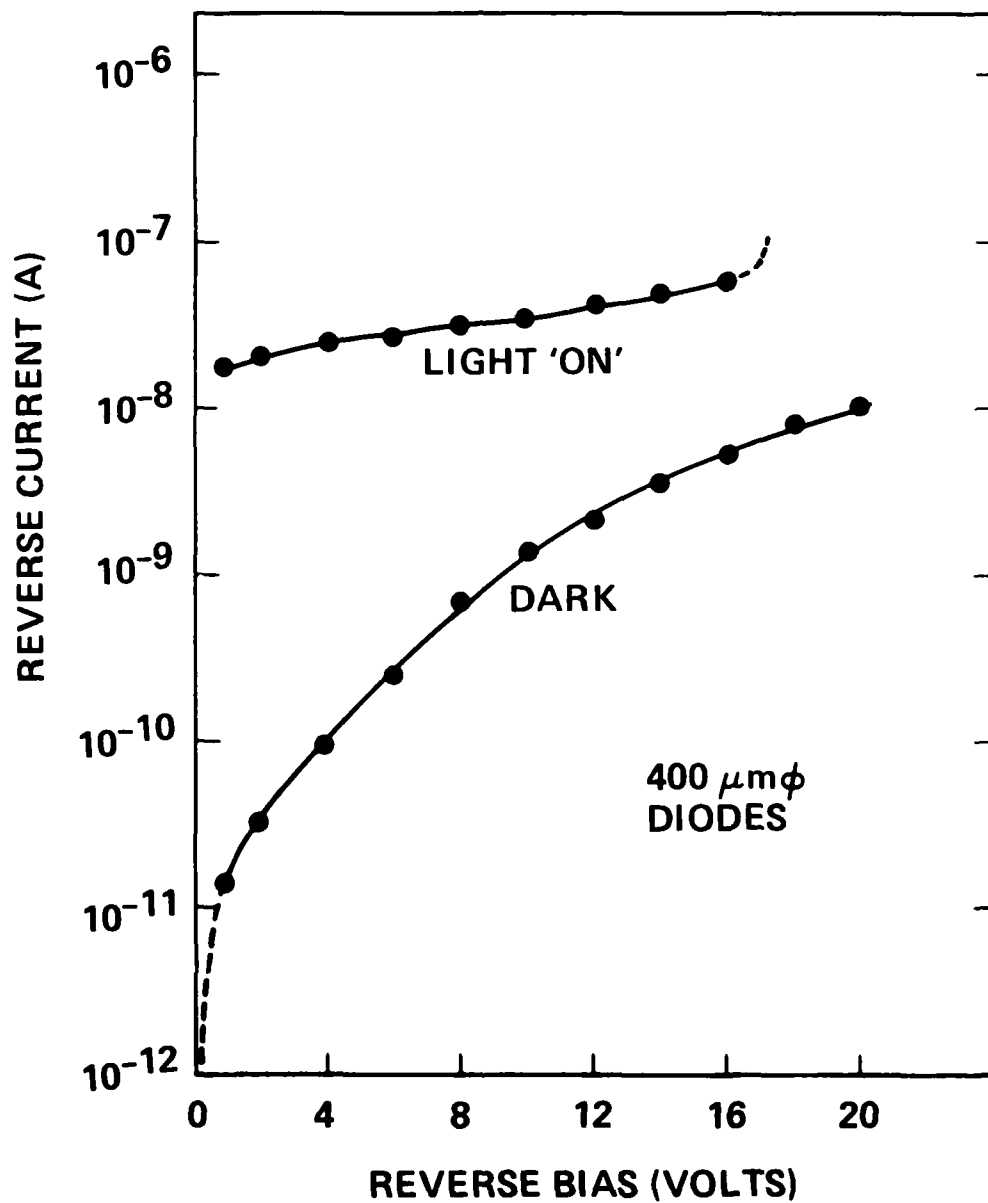


Figure 8. Current-voltage characteristics of 400- μm -diameter reverse-biased Schottky diodes on p-InP.

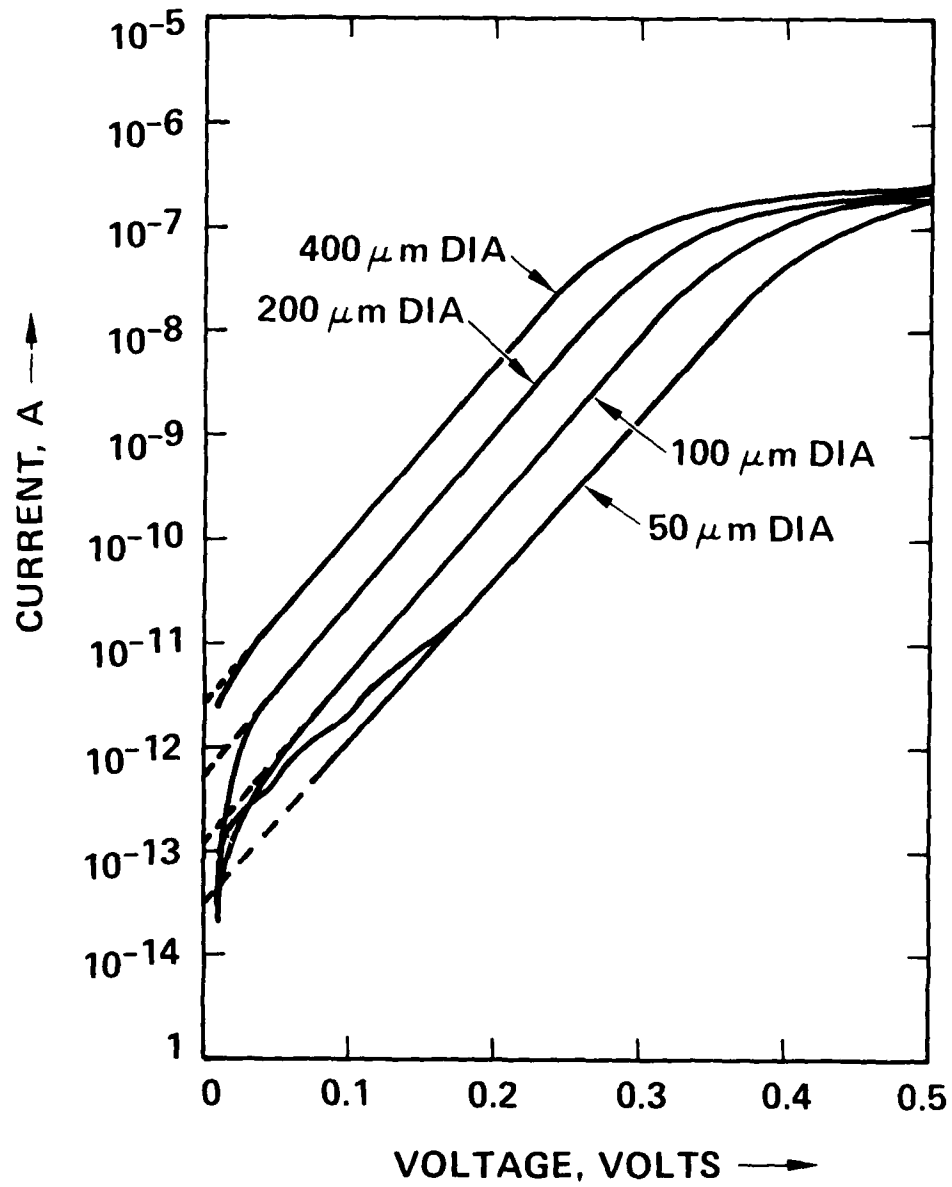


Figure 9. Current-voltage characteristics of forward-biased Schottky diodes on p-InP. The Schottky metal was Al.

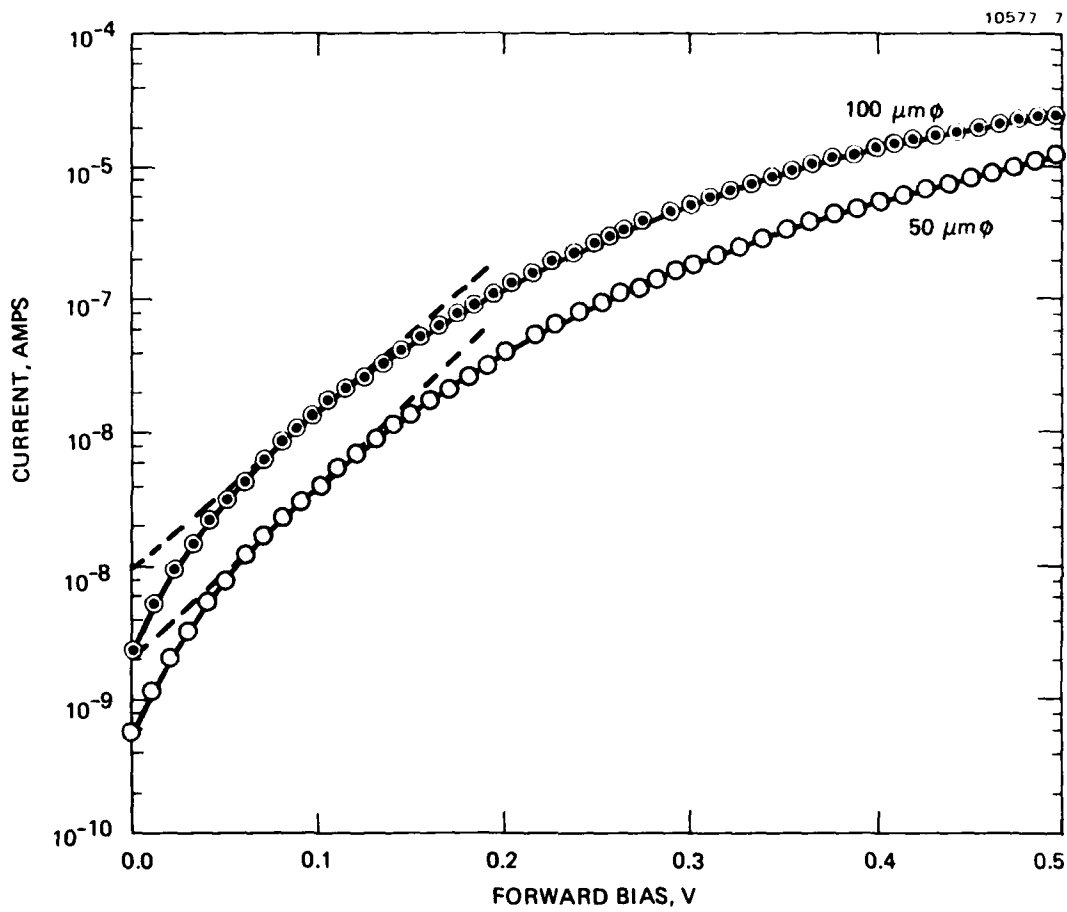


Figure 10. Current-voltage characteristics (forward bias) of Au Schottky diodes on p-InP.

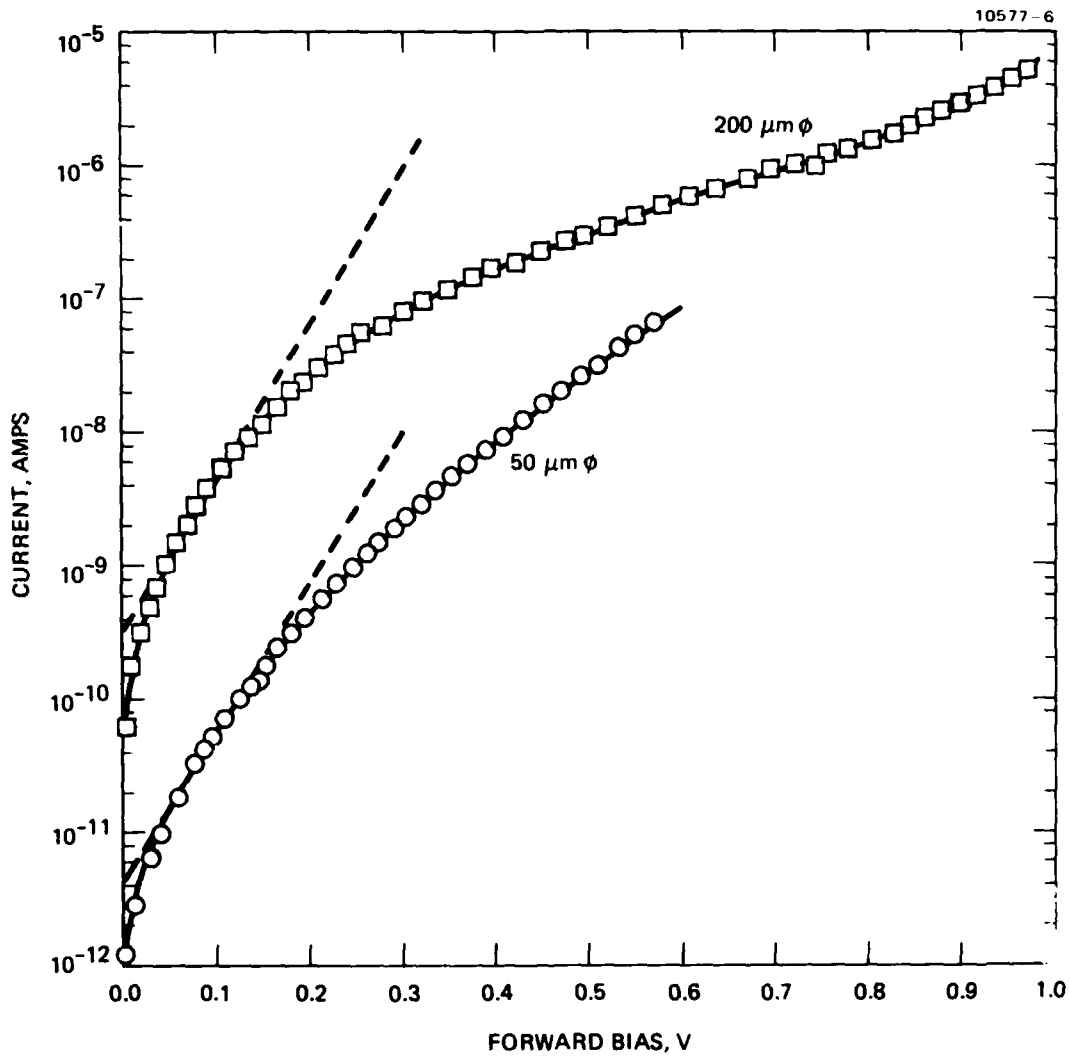


Figure 11. Current-voltage (forward) characteristics of Ag-Schottky diodes on p-InP.

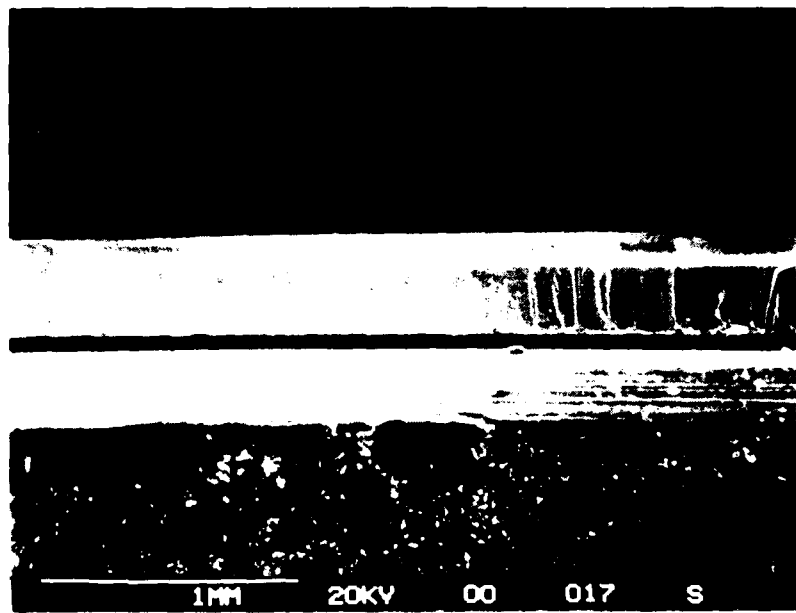


Figure 12(a). SEM micrograph of a mesa etched in InP with mechanically gated 2% solution of bromine in methanol. "Moating" around the edge is clearly evident.

a more uniform etching. The surface of the etched film is smoother than that of jet etching and etching with a 2% solution of bromine in methanol. In adequate thinning, the surface of the etched film is smooth with no evidence of roughness.

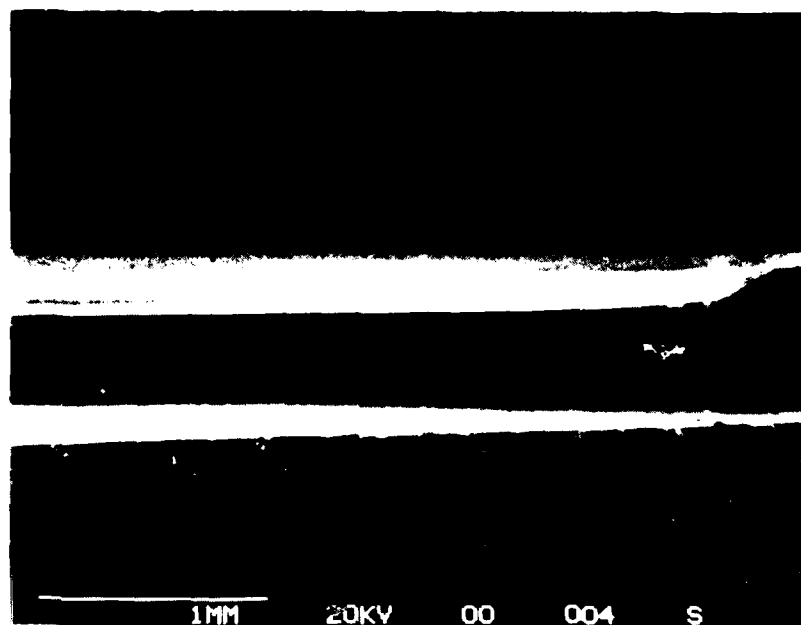


Figure 12(b). SEM micrograph of a specimen produced by jet thinning with a 2% solution of bromine in methanol. The surface is smooth with no evidence of roughness.

SECTION 4

IONIZATION COEFFICIENT MEASUREMENTS

A. DESIGN OF THE EXPERIMENTAL SYSTEM TO PERFORM IONIZATION COEFFICIENT MEASUREMENTS

As discussed in an earlier section, an ideal ionization coefficient measurement experiment must be capable of achieving pure electron and hole injection in the same device rather than in complementary devices. Our experimental system has been designed to satisfy this criterion and does not require the use of a transparent Schottky barrier. The details of the experimental setup are described below.

The pure electron and pure hole injection in our case are achieved by the absorption of 0.638 and 1.152 μm radiations, respectively. The sample in both cases is illuminated from the backside, and the ohmic as well as the Schottky contacts are made from the top surface of the wafer. The 0.638 μm radiation with energy greater than the band gap of InP creates electron-hole pairs near the back surface of the sample, and the minority carriers (in our case, electrons), will be injected into the high-field region (provided the sample is sufficiently thin) avalanche multiplied, and collected by the reverse-biased Schottky. The 1.152 μm radiation, on the other hand, is highly transparent, and consequently, is incident at the metal-semiconductor interface. As a result, holes are injected over the barrier, which in turn are injected into the high-field region, thus achieving pure-electron and pure-hole injection.

The detailed experimental setup is schematically shown in Figure 13. Two stable He-Ne lasers, one capable of operation at 0.6328 μm and the other at 1.152 μm , provide the necessary illumination. Chopped light from the two lasers is focused onto optical fibers, labeled 1 and 2 in Figure 13. The two fibers are fused in the middle, permitting coupling of radiation between the fibers. Approximately 50% of the radiation couples from fiber 1 to fiber 2 and vice versa. Radiation from fiber 2 is focused by a microscope objective onto the device structure, as shown in Figure 13. The radiation from fiber 1 is detected by a reference photodetector and provides a measure of the laser intensity incident on the test device at any given time. This feature will permit us to account for any fluctuations in the laser intensity during the time it takes to complete the measurement. The photo-induced

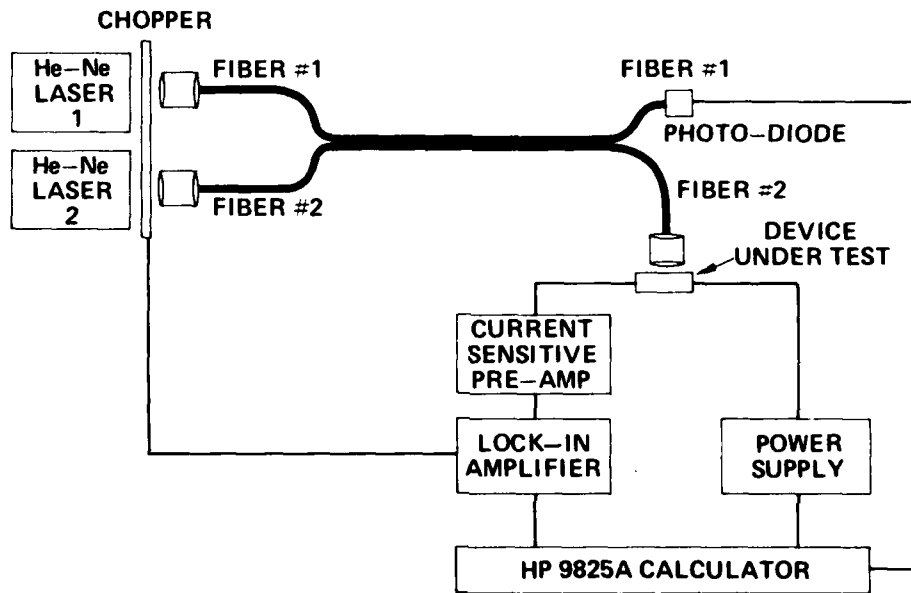


Figure 13. Schematic of the automated photoresponse measurement system.

currents will be measured by a current-sensitive preamplifier and a lock-in amplifier. The voltage applied to the device under test and the measurements will be controlled by a HP 9825A calculator.

B. EXPERIMENTAL MEASUREMENTS

Photoresponse measurements were performed by illuminating the Al Schottky diodes with either 0.6328 μm or 1.152 μm radiation. Figure 14 shows the measured photocurrents as a function of bias. The solid curve represents the data obtained with 1.152 μm radiation (hole injection), while the dashed curve was obtained with 0.6328 μm radiation (electron injection). The data shown were obtained from a 400 μm -diameter diode prior to thinning.

Variations in laser intensity from one measurement to the next can easily be taken care of by plotting the ratio of the photocurrent at a bias ($I(V)$) to the photocurrent at zero bias ($I(0)$). The normalized photocurrent due to hole injection ($I(V)/I(0)$) is plotted in Figure 15. The relative photoresponse increases continuously as a function of bias. The multiplication factor (M_p), is defined as the ratio of the total current to the injected hole current. It is therefore extremely important to know the injected hole current or the hole base-line current as a function of the applied bias. Van Overstraeten and DeMan⁷ suggest the use of the zero bias current to obtain M_p . This assumes that the unmultiplied photocurrent is independent of the bias. This is a poor approximation. Lee et al.⁸ suggest the use of a linearly extrapolated base line as shown by a dotted line in Figure 15. We have used this approximation, even though it is not very accurate. The multiplication factor caused by holes (M_p) is plotted in Figure 16. More recently, Kao and Crowell⁹ have successfully obtained the baseline for majority carrier injection by considering image force lowering, phonon scattering, and field dependence of quantum mechanical transmission effects. By using an effective phonon scattering mean-free path ($\lambda_e = 34 \text{ \AA}$) and fitting the low-field portion of the measured majority photocurrent, Kao and Crowell⁹ have obtained a good baseline for the majority photocurrents. We will use this approach in our evaluations of the baseline photoresponse as soon as measurements on suitable device structures are available.

The minority carrier (electron) initiated photocurrent is plotted as a function of applied reverse bias in Figure 17. The electron injection was achieved by illuminating the sample with the 0.6328 μm laser. The data

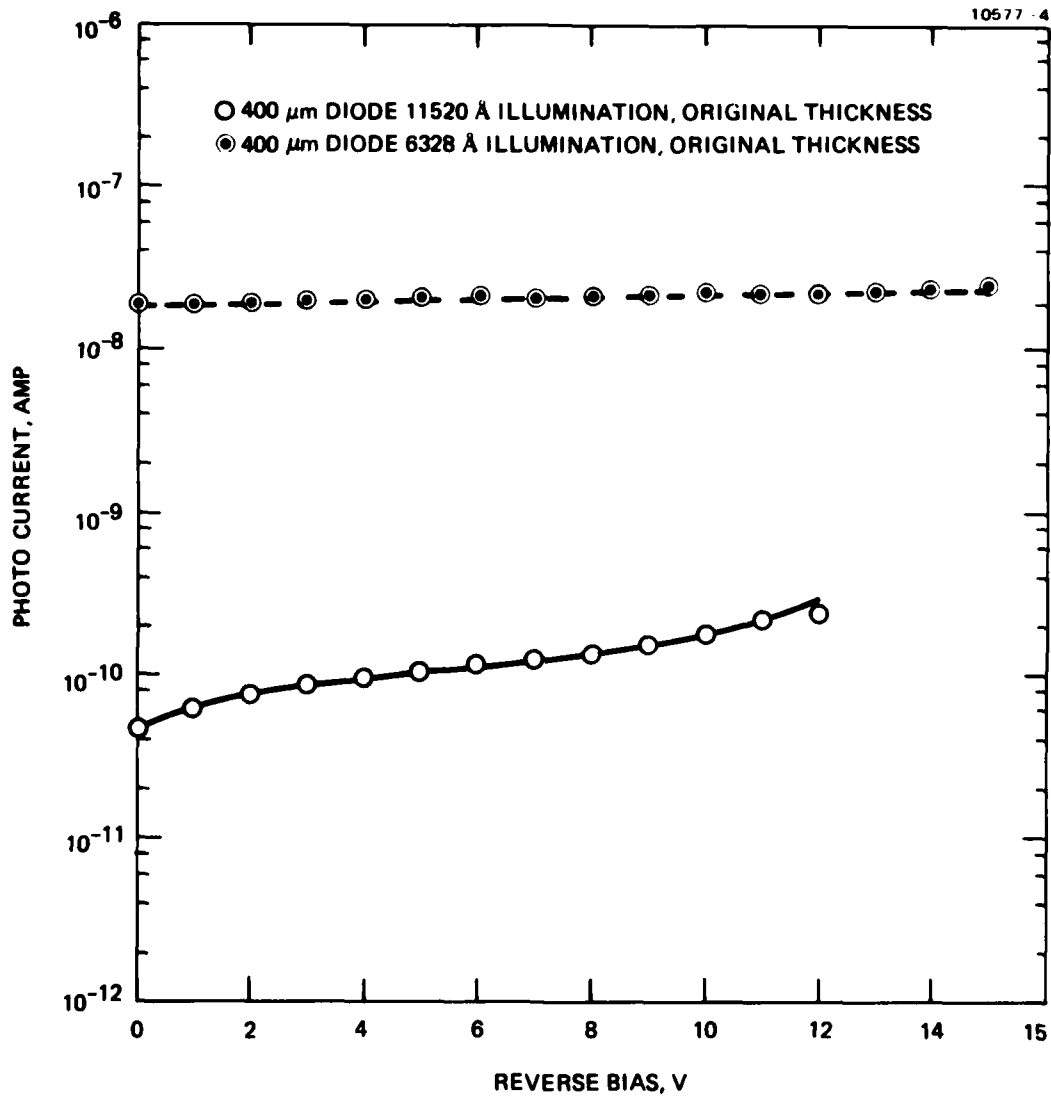


Figure 14.

The measured photocurrents as a function of reverse bias from a 400 μm diameter Schottky diode on p-InP. The dashed curve represents photocurrent caused by 0.6328 μm illumination while the solid curve represents photocurrent caused by 1.152 μm illumination.

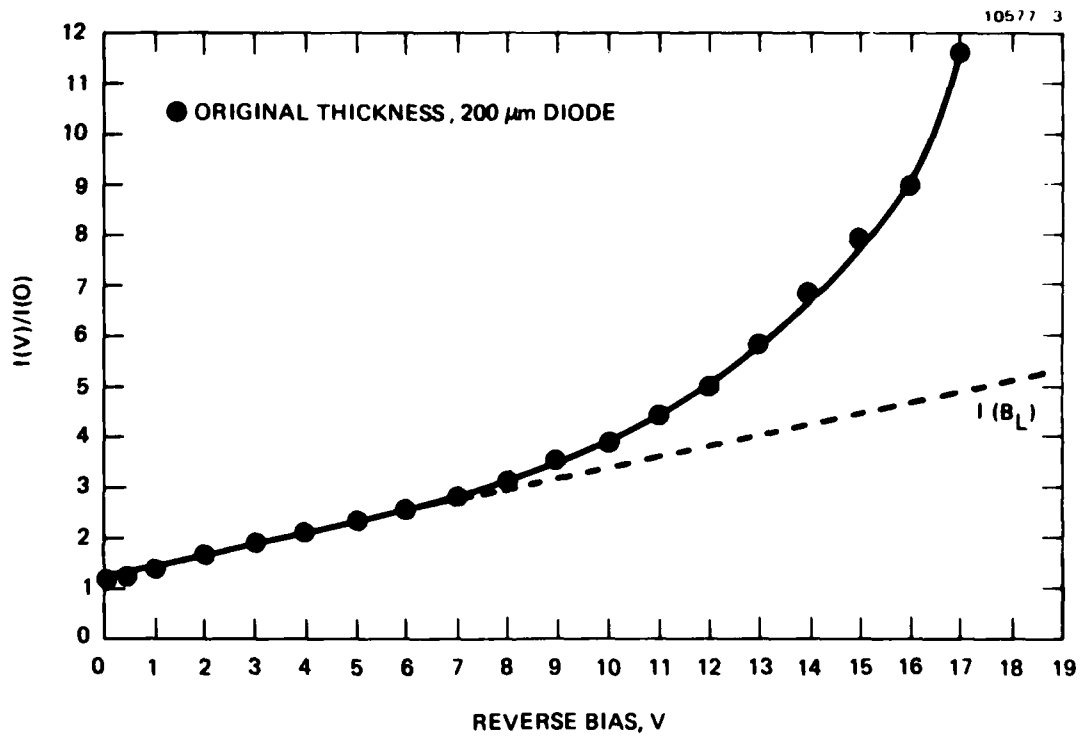


Figure 15. Normalized photocurrent due to 1.152 μm illumination on p-InP. The dashed curve represents linearly extrapolated, nonmultiplied base line photocurrent.

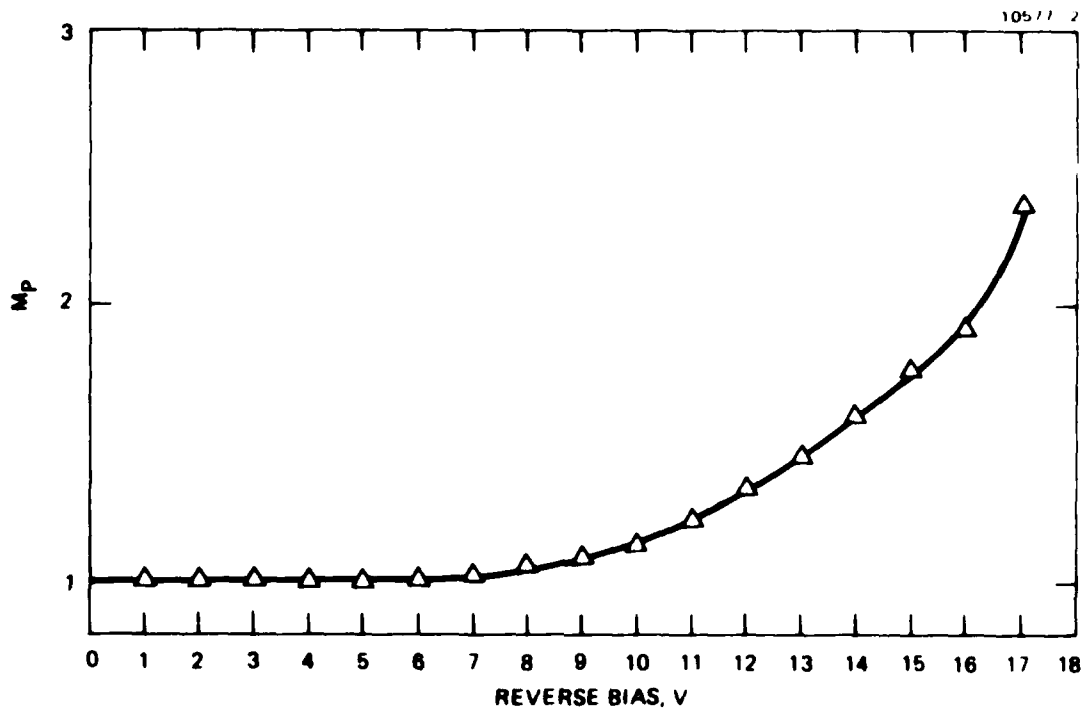


Figure 16. Hole-initiated avalanche multiplication factor obtained from p-InP diodes. The calculations assume linearly extrapolated nonmultiplied base line photocurrents.

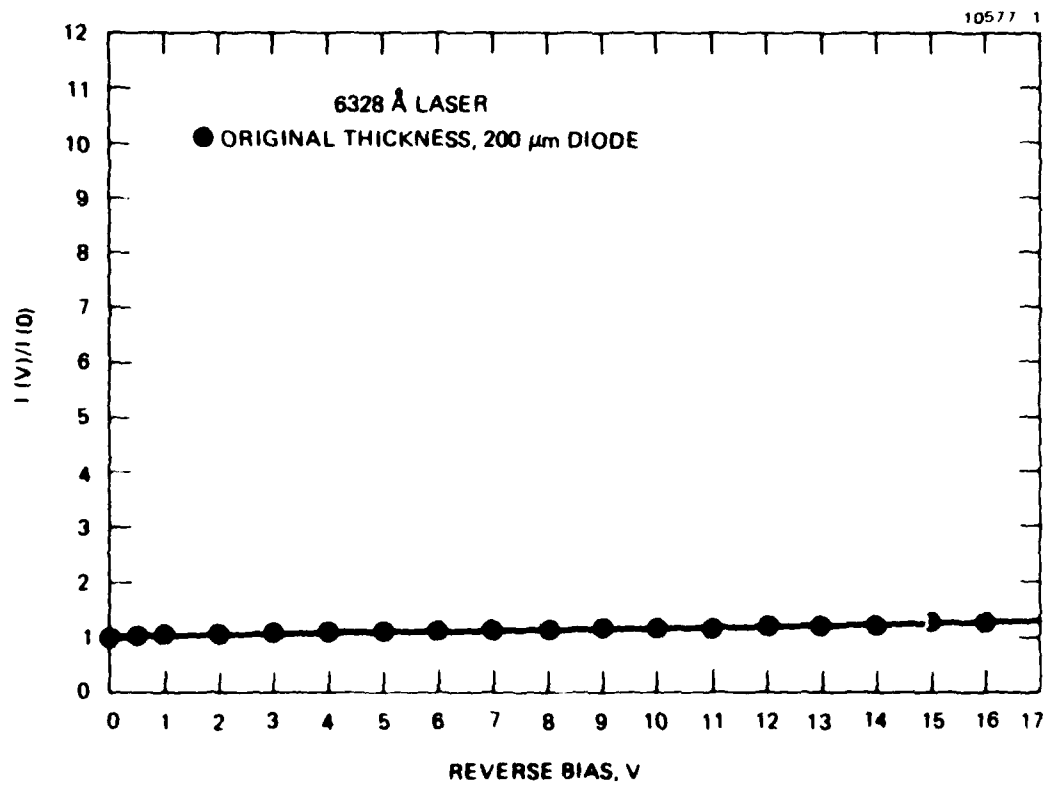


Figure 17. Normalized photocurrent caused by 0.6328 μm illumination on p-InP.

clearly show no evidence of multiplication over the range of bias voltage studied. The reason for lack of multiplication is probably because the sample is several times thicker than the minority carrier diffusion length. Thus the photo-induced electrons do not reach the high-field region. It is essential to thin the sample to observe the electron multiplied photocurrent. During the thinning process, this sample shattered thus precluding any further measurements. This mechanical problem can be easily overcome by mounting the sample to an appropriate fixture to relieve any stress developed during thinning and handling. We are in the process of fabricating devices to meet this goal.

SECTION 5

SUMMARY

The results discussed in the previous sections of this report are summarized below.

In the area of epitaxial growth, high-purity n-type layers with carrier concentrations of $3 \times 10^{15} \text{ cm}^{-3}$ and room temperature mobilities of $5,000 \text{ cm}^2 \text{ V}^{-1} \text{ sec}^{-1}$ with excellent surface morphology can be grown reproducibly using the infinite solution growth technique. To grow layers with such properties, it is necessary to introduce small quantities (v1 ppm) of water vapor in the growth ambient. The presence of water vapor in the growth ambient suppresses the reduction of quartz to silicon by the hydrogen present in the growth ambient. This minimizes the silicon doping of the solution and the epitaxial layers. Auger electron spectroscopy (AES) and secondary ion mass spectrometry (SIMS) measurements show the presence of a higher concentration of Si in the epitaxial layers grown in the absence of water vapor. The SIMS data also reveal the presence of S in these layers. Thus a detailed explanation of the measured electrical and photoluminescence properties of the epitaxial layers involves the interaction between Si and S, the two dominant residual impurities.

Schottky diodes with Al, Ag, and Au as barrier metals were fabricated on highly doped p-type InP by conventional photolithographic techniques. All of these diodes exhibited low leakage currents and abrupt breakdown characteristics. From the I-V characteristics of these devices, we estimate the Schottky barrier heights to be 0.9, 0.74, and 0.64 eV, respectively. Al appears to be the best Schottky metal for fabricating test device for performing ionization coefficient measurements.

A computer-controlled system capable of performing photocurrent measurements as a function of bias has been assembled. The necessary software for performing these automated measurements have developed. Photo-response measurements on Al Schottky diodes on p-type InP have been performed with both 0.6328 and 1.152 μm illumination. Analysis of the data reveals that photomultiplication has been obtained when the sample is illuminated with 1.152 μm radiation (majority carrier initiated

multiplication). Failure to observe minority carrier initiated multiplication is attributed to the sample being too thick, compared with the minority carrier diffusion length. A jet-etching technique to uniformly thin the test device has been developed.

REFERENCES

1. S.H. Groves and M.C. Plonko, Institute of Physics Conference, Series No. 45, p. 71 (1978), and references therein.
2. R.C. Clarke, Institute of Physics Conference Series No. 45, p. 19 (1978), and references therein.
3. J.P. Duchemin, M. Bonnet, G. Benchet, and F. Koeloch, Institute of Physics Conference Series No. 45, p. 10 (1978), and references therein.
4. L. Frass and K. Zanio, J. Electronic Materials 7, 221 (1978).
5. J.H. McFee, B.I. Miller, and K.J. Bachman Journal of Electrochemical Society 124, 259 (1977).
6. A.G. Chynoweth, in Semiconductors and Semimetals, R.K. Willardson and A.G. Beer Eds., Vol. 4 (Academic Press, 1968).
7. R. Van Overstraeten and H. DeMan, Solid State Electronics. 13, 583 (1970).
8. C.A. Lee, R.A. Logan, R.L. Batdorf, J.J. Kleimack, and W. Wiegmann, Phys. Rev. 134, A 761 (1964).
9. C.W. Kao and C.R. Crowell Solid State Electronics 23, 881 (1980).

DATE
ILMED
-8